CORE
Metadata, citation and similar papers at core.ac.uk
Provided by e-Prints Soton

The $\tilde{A}\leftarrow\tilde{X}(1+1)$ REMPI spectrum and high-level *ab initio* calculations of the complex between NO and N_2

Jérôme Lozeille, Sophia E. Daire, Stuart D. Gamblin, and Timothy G. Wright[a)]
Spectroscopy of Complexes and Radicals (SOCAR) Group, School of Chemistry, Physics and Environmental Science, University of Sussex, Falmer, Brighton, BN1 9QJ, United Kingdom

Edmond P. F. Lee
Department of Chemistry, University of Southampton, Highfield, Southampton, SO17 1BJ, United Kingdom and Department of Applied Biology and Chemical Technology, Hong Kong Polytechnic University, Hung Hom, Hong Kong

(Received 11 August 2000; accepted 26 September 2000)

The results of two separate studies of the complex between NO and N_2 are reported. The (1+1) REMPI spectrum of the $\tilde{A}\leftarrow\tilde{X}$ transition of the complex between NO and N_2 is presented of improved quality over that reported previously, and the appearance of the spectrum is discussed. The results of high-level *ab initio* calculations [RCCSD(T)/aug-cc-pVQZ//QCISD/6-311+G(2d)] on the $\tilde{X}\,^2\Pi$ state are also reported. The indications are that the NO moiety is more freely rotating in the complex than is N_2, and that a wide angular space is sampled in the zero-point energy level. The appearance of the REMPI spectrum suggests that the $\tilde{A}\,^2\Sigma^+$ state is (close to) linear, and RCCSD(T)//QCISD calculations on the $\tilde{A}$ state, using Rydberg-function-augmented basis sets, suggest that the lowest energy linear isomer is the $ON\cdot N_2$ linear orientation. It is clear, however, that the understanding of this complex, and its spectroscopy, is far from complete, and will be challenging. © *2000 American Institute of Physics.* [S0021-9606(00)00548-1]

I. INTRODUCTION

The study of the electronic spectroscopy of complexes consisting of a closed-shell atom and an open-shell diatomic has received a considerable amount of attention over recent years, with the majority of studies concentrating on complexes of a rare gas atom (Rg) and the diatomic hydrides, OH, SH, NH and CH.[1–4] There has also been an increasing interest in complexes of Rg with the stable open-shell molecule NO (see the recent references, Refs. 5–9, and references cited therein). These studies have served as an impetus to the development of new spectroscopic theory in order to understand fully the observed spectra.

As well as closed-shell atoms complexed to open-shell diatomics, work has also been developing on the electronic spectroscopy of closed-shell diatomics and polyatomics complexed to open-shell diatoms. For the diatomic hydrides, this is almost exclusively the work on the $H_2\cdot OH$ complex,[10] although work has also commenced upon the $CH_4\cdot OH$ complex.[11] Regarding NO-containing complexes, reports of electronic spectra of ''$NO\cdot N_2$,''[12] $NO\cdot CH_4$,[13,14] and $NO\cdot C_2H_6$[15] have been made.

It should be noted at this point that the most detailed results on the ground $\tilde{X}\,^2\Pi$ state (where the nomenclature implies that the complex involves interaction with NO in the $X\,^2\Pi$ state) have come from microwave/radiofrequency and infrared experiments. $Ne\cdot NO$[16,17] and $Ar\cdot NO$[18] have been the subject of microwave/radiofrequency experiments and more recently, IR/UV double-resonance studies combined with good quality *ab initio* potential energy surfaces.[19–22] To our knowledge, the only example of NO complexed to a molecule that has been studied at this resolution is the $NO\cdot HF$ complex, which has been studied by infrared[23] and microwave[24] spectroscopy.

Recently, we have been undertaking a study of the $\tilde{A}\leftarrow\tilde{X}$ transitions of NO-containing complexes using resonance-enhanced multiphoton ionization (REMPI) spectroscopy employing a new apparatus, recently built at Sussex. We have been producing spectra that are either much improved over previously recorded spectra, or completely new. In the present work, we report our improved spectra of the $\tilde{A}\leftarrow\tilde{X}$ transition of the complex formed between NO and N_2.

In order to understand the spectroscopy of these species, it is often useful to combine the experimental study with *ab initio* results. Unfortunately, the excited states of the NO-containing species are somewhat difficult to study theoretically, but good progress is being made on the $\tilde{X}$ states, with high-quality potential energy surfaces (PESs) available for $He\cdot NO$,[25] $Ne\cdot NO$,[20] and $Ar\cdot NO$.[26] There appear to be no detailed *ab initio* results involving NO complexed to a polyatomic, although there are two reports on aspects of the energy minima of the $NO\cdot H_2O$ complex,[27,28] which indicate that these calculations are highly challenging for the ground state—the excited states are expected to be even more demanding. However, if such calculations can be performed reliably, then some insight can be gained into the $\tilde{X}$ state, which will help to start to elucidate the spectroscopy that is

a)Author to whom correspondence should be addressed. Fax: +44 1273 677196; electronic mail: t.g.wright@sussex.ac.uk

Downloaded 17 Nov 2009 to 152.78.208.72. Redistribution subject to AIP license or copyright; see http://jcp.aip.org/jcp/copyright.jsp

observed. With this in mind, we also present in this work, high-level *ab initio* calculations of the complex between N_2 and NO in the ground electronic state ($\tilde{X}\,^2\Pi$), together with calculations on the linear isomers of the $\tilde{A}$ state. Note that in the following, we use the notation $\{NO\}\cdot N_2$ to indicate that the orientation of the NO is not implied; in cases where the brackets are missing, the orientation is implied (so that $NO\cdot N_2$ implies that the oxygen atom is directed towards the N_2 molecule).

II. EXPERIMENT

The apparatus consists of a two-chamber vacuum system: the first vacuum chamber contains the molecular beam source (Parker/General Valve; 750 μm diameter orifice), and is pumped by a 3000 ls^{-1} diffusion pump (Leybold DIP 3000), backed by a 40 m^3h^{-1} rotary pump (Leybold TRIVAC D40B); the second chamber is the ionization chamber, and contains the ion/electron extraction system, as well as two time-of-flight tubes. For these experiments the chambers were simply connected, and the free jet expansion was unskimmed. The main ionization chamber is pumped by a 1000 ls^{-1} turbomolecular pump (Leybold TURBOVAC 1000 C, backed by a second 40 m^3h^{-1} rotary pump), positioned directly in the line of sight of the molecular beam expansion. In addition, two small (150 ls^{-1}) turbomolecular pumps (Leybold TURBOVAC 151) are present, backed by a single rotary pump (Leybold TRIVAC D10E), each pumping one of the time-of-flight tubes. For the experiments reported here, only one of the time-of-flight tubes is employed to detect ions (the other time-of-flight tube is intended for the detection of electrons). At the end of this tube is a dual microchannel plate (chevron) detector, which amplifies the ion signal. The signal is passed to an oscilloscope (LeCroy LT342 Waverunner) for monitoring and to a boxcar (SRS SR250) for averaging; the signal from the boxcar is then passed via a computer interface (SRS SR245) to a PC for storage and analysis.

The laser radiation for the experiments is generated from an excimer-pumped (Lumonics Pulsemaster 842) dye laser (Sirah CobraStretch operating on Coumarin 450), which is frequency doubled, steered and focused (250 mm, slightly defocused) into the center of the ionization region. Ions formed are extracted and focused along the time-of-flight tube for detection. Timings are carried out using a digital delay generator (SRS DG535). Owing to problems with large NO^+ parent signals, development of the detection electronics, and recording of spectra as early a possible in the molecular beam pulse, was necessary. Even so, sometimes contamination of the spectrum of the complex by small amounts of the NO signal occurred, but in these cases was easily subtracted by recording background spectra close to the $\{NO\}^+\cdot N_2$ time of flight; the subtraction was found to be essentially exact. In this way, we are able to ensure that the spectra presented herein are clean.

$\{NO\}\cdot N_2$ complexes were formed by a pulsed (10 Hz, 300 μs) supersonic expansion of a mixture of 1% NO in argon, to which had been added various amounts of N_2. It was found that mixtures very rich in N_2 could be used, although when they were too rich the spectra became less resolved (presumably as rotational cooling became less efficient). The optimum concentration of N_2 was found to be ca. 20%. The coldest spectra were recorded, as ever, at the front of the sharpest gas pulses.

Calibration was performed by comparing measured cold NO $A\leftarrow X$ line positions with those calculated from the spectroscopic constants given by Danielak *et al.*,[29] which were in excellent agreement with those from an older compilation,[30] additionally, we confirmed our calibration against two Xe resonances observed in previous work.[8] We estimate an absolute precision of ± 0.3 cm^{-1}, with differences accurate to ± 0.1 cm^{-1}.

III. COMPUTATIONAL DETAILS

In performing calculations on a weakly-bound complex that contains a significant number of electrons, one is usually forced to compromise, owing to the expense of the calculations. Ideally, of course, convergence of the calculated quantities with both the basis set and level of theory would be achieved; however, this is usually impractical. Extrapolation to the complete basis set limit has been used in a number of cases; however, we are wary of such schemes for weakly-bound species, as they have often only been tested on a small number of molecules, some of which are not characteristic of the complex under study. In the present work, we optimize the geometry and obtain vibrational frequencies at the highest practicable level of theory, and then perform single-point calculations at that geometry in order to obtain more accurate energy differences. This procedure will lead to the most reliable results when the potential energy surface is rather flat, since then small changes in geometry lead to only small changes in energies at the same level of theory. (Thus, the fact that the optimized geometry at the highest level of theory used for the single-point calculations would be slightly different from that obtained at the highest level of theory used for the geometry optimizations is not important.)

A. $\tilde{X}$ state

Geometry optimizations were performed at levels of theory ranging from MP2/6-31+G* to QCISD/6-311+G(2d). We considered a number of possible geometric isomers: linear ($ON\cdot N_2$ and $NO\cdot N_2$); the lowest $^2B_1$ and $^2B_2$ electronic states in a T-shaped orientation ($NO\cdot N_2$ and $ON\cdot N_2$)—where the $^2B_2$ state has the unpaired electron in-plane; and a nonplanar, ''X'' type structure. For the latter, in principle, there are A' and A'' states, but we found that the A'' state always optimized back to a T-shaped structure. A slipped parallel structure was also considered, but this also always reverted back to a T-shaped structure. It was found that the energy ordering of these states was not consistent, even up to the highest level of theory used for the geometry optimizations. We thus decided to take the geometries at this [QCISD/6-311+G(2d)] level of theory and to perform single-point RCCSD(T)/aug-cc-pVTZ and aug-cc-pVQZ single-point calculations on these. The interaction energies were corrected for basis set superposition error (BSSE) using the full counterpoise correction.[31]

Downloaded 17 Nov 2009 to 152.78.208.72. Redistribution subject to AIP license or copyright; see http://jcp.aip.org/jcp/copyright.jsp

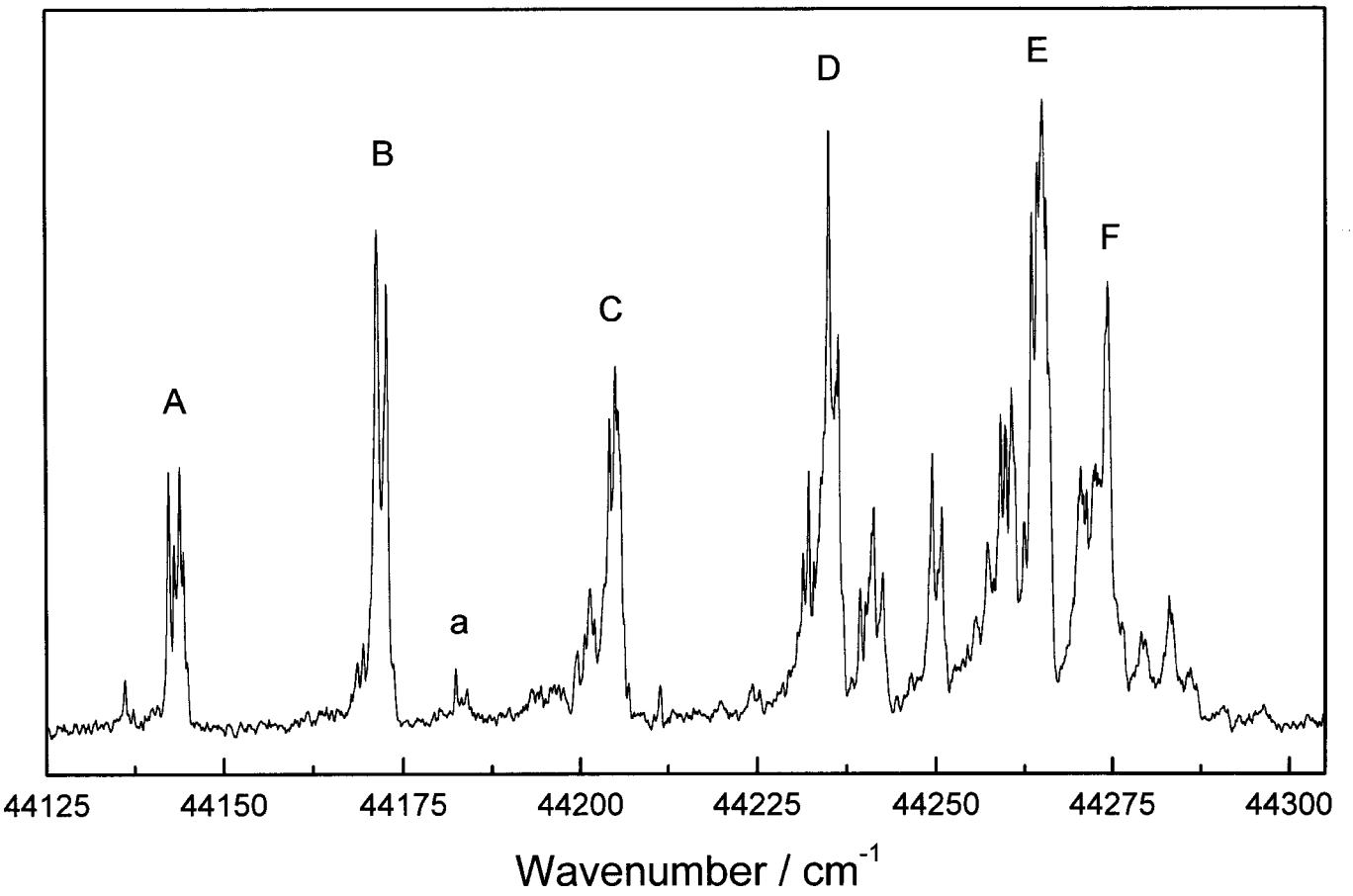

FIG. 1. Overview (1+1) REMPI spectrum of the $\tilde{A}\leftarrow\tilde{X}$ transition of $\{NO\}\cdot N_2$.

Geometry optimizations were performed employing GAUSSIAN 98;[32] single-point RCCSD(T) calculations were carried out using MOLPRO.[33]

B. $\tilde{A}$ state

It turned out that it was useful to perform calculations also on the $\tilde{A}$ state of $\{NO\}\cdot N_2$, where N_2 is bound to the $A\,^2\Sigma^+$ state of NO. This state corresponds to an electron having been excited to the 3*s* Rydberg orbital on NO, and so these calculations required the use of extra diffuse functions on the NO moiety in order to allow a description of the 3*s* orbital, and its distortion under complexation.. For the geometry optimizations, we used the 6-311+G(2d) basis set, as before, but augmented it with *s*, *p* and *d* ''Rydberg'' functions with the following exponents: 0.028, 0.025, 0.015 on N; and 0.032, 0.028, and 0.015 on O (from Ref. 34). Since we required geometry optimization and vibrational frequencies, the highest practicable level of theory was QCISD.

In order to obtain more reliable energy differences, single-point energy calculations were also performed at the RCCSD(T) level at the QCISD geometries, employing the aug-cc-pVTZ basis set, augmented with Rydberg functions. Two sets of functions were employed:

The first (denoted Ryd-1) was a $sp2d2f$ augmentation with exponents (*s*,0.028;*p*,0.025;*d*,0.0472,0.015; *f*,0.091,0.02275) for N, and (*s*,0.032;*p*,0.028;*d*,0.0594, 0.015;*f*,0.125,0.03125) for O.

The second (denoted Ryd-2) was a $2s2p2d2f$ augmentation, with exponents (*s*,0.028,0.009333;*p*,0.025,0.008333; *d*,0.0472,0.015;*f*,0.091,0.02275) for N, and (*s*,0.032, 0.010666;*p*,0.028,0.009333;*d*,0.0594,0.015;*f*,0.125,0.03125) for O.

At this point we note that for linear geometries, the lowest state of Σ^+ symmetry is the $\tilde{A}$ electronic state, but that for nonlinear geometries, the $\tilde{X}\,^2\Pi$ state splits into B_1 and B_2 components (C_{2v}) or A' and A'' components (C_s) symmetry. Attempts at converging the excited state at these nonlinear geometries proved difficult, and was abandoned; in all cases it was found that convergence to one of the components of the $\tilde{X}$ state always occurred. We anticipate that accurate calculations on this excited state will require MRCI-based methods, and these are planned for the future. As will be seen from the discussion below, however, the linear excited states appear to be of the main importance here.

IV. RESULTS

A. (1+1)REMPI spectrum of the $\tilde{A}\leftarrow\tilde{X}$ transition of $\{NO\}\cdot N_2$

Figure 1 shows the one-color REMPI spectrum of $\{NO\}\cdot N_2$ obtained via excitation on the NO moiety, in the region of the $A\leftarrow X$ transition. The spectrum looks very similar to that reported previously by one of the present authors and others[12] in a preliminary communication. The spectrum

Downloaded 17 Nov 2009 to 152.78.208.72. Redistribution subject to AIP license or copyright; see http://jcp.aip.org/jcp/copyright.jsp

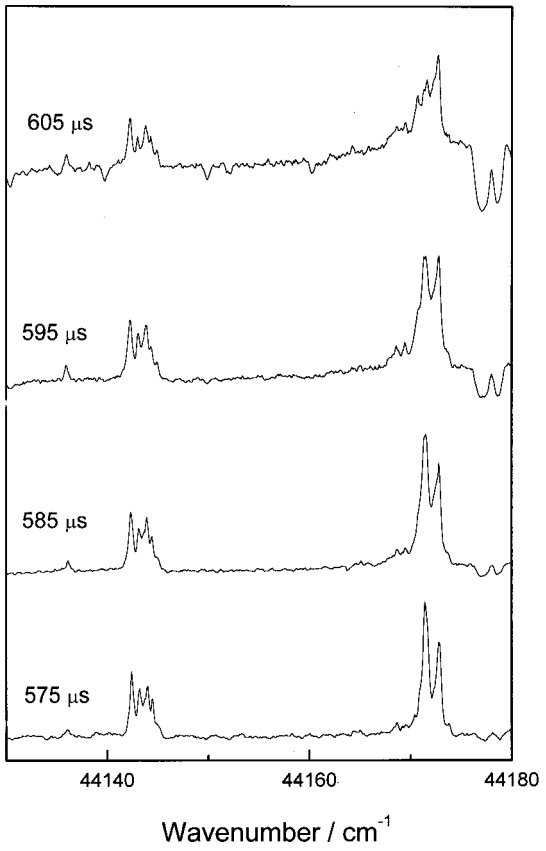

FIG. 2. Effect of laser/pulsed-valve delay on the appearance of the REMPI spectrum of $\{NO\}\cdot N_2$—close up of features A and B. At the longest delays, large interference from NO transitions is observed throughout the spectrum.

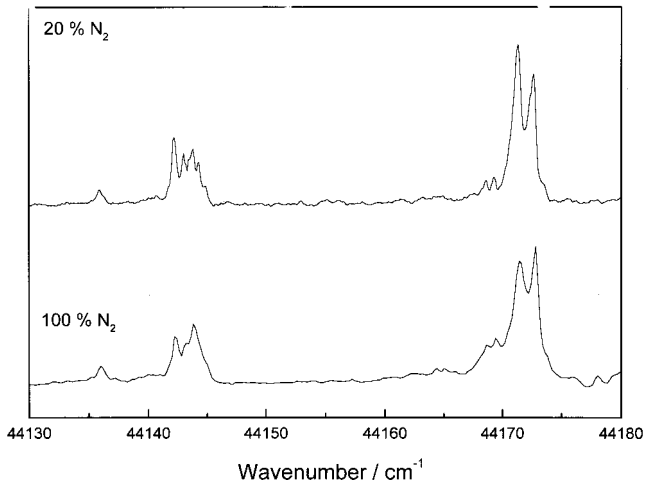

FIG. 3. Features A and B in the $(1+1)$ REMPI spectrum of the $\tilde{A}\leftarrow\tilde{X}$ transition of $\{NO\}\cdot N_2$ recorded using an optimal mix of ~1% NO in 20% N_2 and balance of Ar, and a mix of ~1% NO in pure N_2.

here is, however, of a higher quality, mainly because of a higher resolution. The spectrum was recorded at the front of the gas pulse, but notably, the spectrum appeared to be more or less unchanged as we probed deeper in the pulse, which corresponds to higher internal temperature—see Fig. 2. Eventually, at the longer delays, there appears to be a rotational broadening, and an increased interference from intense warm lines of the $A\leftarrow X$ transition of NO, which arise owing to saturation of the MCPs used for ion detection. Figure 3 shows two spectra recorded with different concentrations of N_2, and it can be seen that for a mixture of NO in pure N_2, the cooling is not as efficient as that of the optimal mixture of 20% N_2 in a balance of Ar, as evinced by the broader line profiles. In addition, we note that apart from $\{NO\}^+\cdot N_2$ we were unable to observe any other ions except NO^+ and $Ar\cdot NO^+$ in this spectral region, under the coldest conditions, which confirms that all of the features in the spectrum arise from $\{NO\}\cdot N_2$, and do not arise, for example, from fragmentation of higher complexes, such as was observed by us in a recent NO/ethane study.[15]

The higher quality of the present spectrum reveals a large number of features that were obscured in the previous work, and show that the spectrum is highly structured and complicated. In particular, the structure of Feature A and Feature B (see Figs. 1–3) is distinctly different, with the origin band consisting of at least five closely-spaced components, with a weak feature to the red, while the second feature appears to consist of two intense features, with some structure to the red. There is a weak feature (labeled a), which is then followed by the strong Features C–G. Note that we have only labeled the strongest features, but it is clear that there is more structure in the spectrum. As noted previously,[12] although the regular spacing of Features A–E tempts one to assign them to a progression, the intensity profile makes such an assignment unlikely; in addition, the different partially-resolved profiles also makes such an assignment unlikely. The feature that does not match the monotonic increase in intensity is Feature C, and there was some uncertainty in Ref. 12 regarding its relative intensity, since it is at almost the same energy as the NO $A\leftarrow X$ origin. In the present work, we have reduced the interference from NO transitions, and are confident that Feature C is indeed weaker than Features B and D. The spacing between the centers of Features A and B is 29 cm^{-1}, and that between Features A and C is 62 cm^{-1}, and the most likely (tentative) assignment is that these are different vibrational modes of the excited state of the complex, α and β, respectively. That Feature D is ~30 cm^{-1} from C tempts one to assign it to a combination band, $\alpha+\beta$. Thereafter, even a tentative assignment is probably unrealistic, as the dissociation limit is being approached, and internal rotation and mixing of bends and stretches is likely to occur.

Owing to the structured nature of the origin peak, it is not clear where to take the T_0 value—we take the center of the main feature at 44 143.5 cm^{-1}. There is a drop in the intensity of the spectrum above 44 275 cm^{-1}, which is interpreted as being due to dissociation. Previously[12] the dissociation limit was taken as the blue edge of the last clear peak, which is measured here at 44 287.1 cm^{-1}, giving the dissociation energy of the $\tilde{A}$ state as $143.6\pm0.5\,cm^{-1}$—in excellent agreement with the previous value.[12] By measuring the shift of the origin from the $Q_{11}(0.5)$ line of NO at 44 198.9 cm^{-1} (Ref. 29), we derive a ground state dissociation energy of $87.7\pm0.5\,cm^{-1}$, which is also in excellent agreement with that reported previously.[12] However, we note that for the $\tilde{A}$ state of $Ar\cdot NO$, it has been demonstrated that there is a sig-

Downloaded 17 Nov 2009 to 152.78.208.72. Redistribution subject to AIP license or copyright; see http://jcp.aip.org/jcp/copyright.jsp

TABLE I. Optimized geometry at the QCISD/6-311+G(2d) level of theory for seven isomers of the $\{NO\}\cdot N_2$ complex, corresponding to an interaction between N_2 and $NO(X\ ^2\Pi)$.

Structure	State	r_{NO}/Å	r_{NN}/Å	$r_{intermolecular}$/Å	E_{tot}/E_h	E_{rel}/cm^{-1}
$NO\cdot N_2$	$^2\Pi$	1.1575	1.0982	O···N=3.4380	−238.982081	0.0
$ON\cdot N_2$	$^2\Pi$	1.1578	1.0982	N···N=3.7726	−238.981779 $(-13.4i,\pi)$	66.3
$NO\cdot(N_2)$[a]	$^2B_2$	1.1575	1.0983	O···N=3.4827	−238.982038	9.4
$NO\cdot(N_2)$[a]	$^2B_1$	1.1576	1.0982	O···N=3.4867	−238.982053	6.1
$ON\cdot(N_2)$[a]	$^2B_2$	1.1575	1.0982	N···N=3.6510	−238.981938	31.4
$ON\cdot(N_2)$[a]	$^2B_1$	1.1574	1.0982	N···N=3.6726	−238.981981	36.0
$(NO)(N_2)$[b]	$^2A'$	1.1575	1.0982	N···O=3.5913	−238.981993	19.3

[a]C_{2v} geometry, with the NO directed to the center of N_2.
[b]Nonplanar ''X''-shaped geometry.

nificant barrier to dissociation,[35] and it is possible that such a barrier exists for $\{NO\}\cdot N_2$ also. In previous work on Kr·NO and Xe·NO,[8] small, weak features were present at the high energy end of the REMPI spectra; in the case of Xe·NO in particular, the dissociation limit seemed clearly identifiable in the spectrum, and so these weak features, which were beyond that limit, must then be attributable to quasibound energy levels. In the present case, we note that the clump of three weak features centered at ca. 44 283 cm^{-1} are significantly weaker than the feature at 44 274.3 cm^{-1}, and it is possible that these are quasibound; if we take the blue edge of this feature (44 275.0 cm^{-1}) as the dissociation limit, then D_0' would then become 131.5 cm^{-1}, leading to $D_0''=76.1\,cm^{-1}$. At the present time, it is not possible to differentiate conclusively between these two possibilities—a photodissociation action spectra, similar to that reported in Ref. 35 for the Ar·NO complex would shed light on these dissociation energies.

B. Results of *ab initio* calculations

1. $\tilde{X}$ state

The calculated equilibrium geometries of the seven lowest geometric isomers at the QCISD/6-311+G(2d) level of theory are presented in Table I, with the calculated harmonic vibrational frequencies in Table II. As may be seen, all geometries correspond to points with all real vibrational frequencies, except for one of the linear isomers (although only one of the π components is imaginary), and the ''X'' shape. It should be noted, however, that the imaginary frequency for the ''X'' shape is very small, and that all of the vibrational frequencies were real at the QCISD/6-31+G* level of theory—see footnote e of Table II. It is plausible, therefore, that the two states with an imaginary vibrational frequency are, in fact, minima on very shallow surfaces. The binding energies obtained from the results of performing single-point RCCSD and RCCSD(T) calculations employing the aug-cc-pVTZ basis set at each of these minima are given in Table III. Table IV contains the same information as Table III, but employing the aug-cc-pVQZ basis set. Test calculations indicated that the BSSE was ca. 40–50 cm^{-1} for the aug-cc-pVTZ basis set, but that fell to 20–25 cm^{-1} for the aug-cc-pVQZ basis set.

The conclusions from these calculations is that the relative energies and binding energies have more or less converged for all of the isomers given the good agreement between the two sets of results in Tables III and IV; it is unlikely that the ordering will change at higher levels of theory. The lowest energy minimum corresponds to an ''X''-shaped isomer, with the T-shaped $^2B_1$ $ON\cdot N_2$ isomer the

TABLE II. Harmonic vibrational frequencies of $\{NO\}\cdot N_2$ calculated at the QCISD/6-311+G(2d) optimized geometries of Table I (b_2 frequencies are in-plane).

Structure	State	Harmonic vibrational frequencies/cm^{-1}					
$NO\cdot N_2$	$^2\Pi$	31.5(σ)	32.3;37.4[a]	73.9;74.2[a]	···	1767.9(σ)[b]	2383.1(σ)[c]
$ON\cdot N_2$	$^2\Pi$	22.0(σ)	$-13.4i$; 24.8[a]	42.7;44.8[a]	···	1761.3(σ)[b]	2383.2(σ)[c]
$NO\cdot(N_2)$[d]	$^2B_2$	23.9b_2	29.6b_1	34.1b_2	35.6a_1	1763.1(a_1)[b]	2382.5(a_1)[c]
$NO\cdot(N_2)$[d]	$^2B_1$	16.0b_2	22.9b_2	29.7b_1	35.7a_1	1764.7(a_1)[b]	2383.4(a_1)[c]
$ON\cdot(N_2)$[d]	$^2B_2$	27.5b_2	28.4b_1	32.1b_2	33.4a_1	1767.4(a_1)[b]	2383.5(a_1)[c]
$ON\cdot(N_2)$[d]	$^2B_1$	6.9b_2	26.9b_1	32.1a_1	33.6b_2	1769.5(a_1)[b]	2383.5(a_1)[c]
$(NO)(N_2)$[e]	$^2A'$	8.7i(a'')	13.8(a'')	34.1(a'')	39.9(a')	1765.7(a')[b]	2383.6(a')[c]

[a]For the linear geometries, the pairs of vibrational frequencies correspond to the π vibrations. These are not completely degenerate owing to the use of unrestricted wavefunctions.
[b]NO stretch vibration.
[c]N_2 stretch vibration.
[d]C_{2v} geometry, with the N_2 moiety crossing the *T*.
[e]Nonplanar ''X''-shaped geometry. Note that small imaginary vibrational frequency at this level of theory. At the QCISD/6-31+G* level of theory, the corresponding vibrational frequencies were all calculated to be real: 15.7, 25.5, 40.7, 46.3, 1932.2, and 2393.1 cm^{-1}.

Downloaded 17 Nov 2009 to 152.78.208.72. Redistribution subject to AIP license or copyright; see http://jcp.aip.org/jcp/copyright.jsp

TABLE III. Calculated relative and binding energies (cm^{-1}) at the RCCSD(T)/aug-cc-pVTZ//QCISD/6-311+G(2d) level of theory.

	E_{rel}		ΔE_e(CP)	
	RCCSD	RCCSD(T)	RCCSD	RCCSD(T)
$NO\cdot(N_2)\ ^2\Pi$	56.8	67.6	−33.9	−54.3
$ON\cdot(N_2)\ ^2\Pi$	70.5	86.3	−17.3	−28.1
$NO\cdot(N_2)\ ^2B_1$	22.4	31.6	−74.9	−96.9
$NO\cdot(N_2)\ ^2B_2$	14.4	21.0	−66.9	−88.9
$ON\cdot(N_2)\ ^2B_1$	0.0	5.3	−81.7	−106.6
$ON\cdot(N_2)\ ^2B_2$	9.1	12.3	−71.0	−96.6
$(NO)\cdot(N_2)\ ^2A'$	0.0	0.0	−89.6	−119.5

next highest in energy. Note, however, that there are very small energy gaps between some of these minima, and that therefore large regions of the angular space will be sampled by the complex. A discussion of these results will be presented below. Unrestricted wavefunctions were used in the geometry optimizations: $\langle S\rangle$ for the $\tilde{X}$ states were ~0.85, while those for the A states were ~0.75.

2. $\tilde{A}$ state

The results of the geometry optimizations for the two linear ($NO\cdot N_2$ and $ON\cdot N_2$) isomers are given in Tables V and VI. (As noted above, it was not possible to perform calculations at nonlinear geometries.) As may be seen, for the $NO\cdot N_2$ isomer (Table V), the geometry is relatively stable with the level of theory, and at the highest level, the NO and N_2 bond lengths match the respective experimental r_e values[36] of 1.0637 Å and 1.094 Å very well. The harmonic vibrational frequencies at the MP2/6-31+G*(Ryd) and QCISD/6-311+G(2d,Ryd) level agree quite well, but the ones obtained at the QCISD/6-31+G*(Ryd) contain a problem with one of the π vibrations; in addition, there is an unphysical NO stretch frequency at the MP2 level of theory. At the QCISD level, however, good agreement is seen with the experimental ω_e values for the NO and N_2 stretch frequencies (2371 and 2360 cm^{-1}, respectively).[36] For the $ON\cdot N_2$ isomer (Table VI), the geometry again seems to be consistent, with the NO and N_2 bond lengths again agreeing closely with the experimental r_e values. This time, the frequencies are relatively consistent, but again the NO stretch frequency is unphysical at the MP2 level—at the QCISD level, however, good agreement is again seen with the experimental ω_e values for the NO and N_2 stretch frequencies.

TABLE IV. Calculated relative and binding energies (cm^{-1}) at the RCCSD(T)/aug-cc-pVQZ//QCISD/6-311+G(2d) level of theory.

State	E_{rel}		ΔE_e(CP)	
	RCCSD	RCCSD(T)	RCCSD	RCCSD(T)
$NO\cdot(N_2)\ ^2\Pi$	56.2	65.9	−36.0	−57.1
$ON\cdot(N_2)\ ^2\Pi$	78.2	95.4	−19.1	−30.3
$NO(N_2)\ ^2B_1$	22.1	21.3	−78.2	−101.4
$NO\cdot(N_2)\ ^2B_2$	23.4	30.5	−70.2	−93.5
$ON\cdot(N_2)\ ^2B_1$	4.3	10.2	−84.3	−110.4
$ON\cdot(N_2)\ ^2B_2$	15.4	20.2	−73.9	−100.7
$(NO)\cdot(N_2)\ ^2A'$	0.0	0.0	−94.0	−125.8

At the QCISD/6-311+G(2d,Ryd) level, the $ON\cdot N_2$ isomer is the more stable by 269 cm^{-1}. Single-point RCCSD/aug-cc-pVTZ(Ryd-1) and RCCSD(T)/aug-cc-pVTZ(Ryd-1) calculations (all BSSE corrected) lead to binding energies of 199 and 230 cm^{-1}, respectively; using the larger Ryd-2 augmentation led to dissociation energies of 201 and 231 cm^{-1}, indicating that these values are close to convergence at the RCCSD(T) level using the aug-cc-pVTZ basis set. The close agreement between the QCISD/6-311+G(2d,Ryd) and these RCCSD(T) results suggest that this binding energy is close to convergence. At all levels of theory, the $NO\cdot N_2$ isomer was calculated to be unbound after BSSE correction. The BSSE for the $\tilde{A}$ state is significant at just under 200 cm^{-1} (more or less equally split between NO and N_2)—this clearly leads to the conclusion that the value for the calculated binding energy should only be viewed as qualitative. An examination of the electronic wavefunction in the ghost center calculations suggested that for the $NO\cdot N_2$ state in particular there is mixing of the N_2 orbitals into the NO 3s Rydberg orbital. It is clear that an even larger Rydberg augmentation might be required here, perhaps with a redesign of other aspects of the basis set.

V. DISCUSSION

A. The assignment of the spectrum

The assignment of the carrier of all of the features in the REMPI spectrum to the $\{NO\}\cdot N_2$ complex rests upon two main facts: the appearance of the spectrum remained more or less unchanged for a range of laser/pulsed valve delays, and also with various mixtures; and second that only $\{NO\}^+\cdot N_2$ ions were of significant intensity over the spectral region scanned. The interpretation of the cutoff in intensity to higher energy as the dissociation limit is consistent with the cutoffs seen in previous studies on $Rg\cdot NO$ complexes. These facts lead to the conclusion that the observed REMPI spectrum exhibits features giving information on all of the energy levels of the complexes from the zero-point through to the dissociation limit.

In order to try to understand the appearance of the spectrum observed, one must first consider the $\tilde{X}$ state. It is clear from the *ab initio* results that, although the global minimum is calculated to be an ''X''-shaped structure, there are several isomers close in energy, which would be accessible with just the zero-point vibrational energy. This indicates that the motion is quite floppy, and that the idea of an ''equilibrium geometry'' is of limited use. Although we have not explicitly calculated the barriers between the minima, the proximity of these minima in energy, together with the low values for the vibrational frequencies, indicates that these barriers are expected to be low. Considering a T-shaped complex of C_{2v} symmetry, in order to go from this structure to the ''X''-shaped structure, the NO must rotate out-of-plane (see Fig. 4). Indeed, the minima next highest in energy all correspond to T-shaped structures. In addition, as noted above, attempts to converge slipped parallel structures led to T-shaped structures—this would correspond to NO rotating in-plane having a very low barrier; also the $NO\cdot N_2$ and $ON\cdot N_2$ isomers are close in energy; these are linked by an in-plane

Downloaded 17 Nov 2009 to 152.78.208.72. Redistribution subject to AIP license or copyright; see http://jcp.aip.org/jcp/copyright.jsp

TABLE V. Optimized geometries and harmonic vibrational frequencies of the linear $ON\cdot N_2$ $\tilde{A}^2\Sigma^+$ isomer at different levels of theory.

Method	Basis	r_{ON}/Å	r_{NN}/Å	$r_{N\cdots N}$/Å	Frequencies/cm^{-1}
MP2	6-31+G*[a]	1.0931	1.1306	3.1319	42.8(π); 67.5(σ); 81.7(π); 2335.0(σ);[d] 5479.8(σ)[c]
MP2	6-31+G*[b]	1.0932	1.1307	3.1301	36.3(π); 67.0(σ); 83.6(π); 2340.5(σ);[d] 5484.1(σ)[c]
QCISD	As above	1.0843	1.1148	3.2278	43.0(π); 53.2(σ); 78.9(π); 2375.0(σ);[c] 2393.7(σ)[d]
MP2	6-31+G*(Ryd)[e]	1.0937	1.1303	3.0789	37.6(π); 62.8(π); 74.3(σ); 2366.8(σ);[d] 5057.3(σ)[c]
QCISD	As above	1.0837	1.1147	3.1451	41.4(π); 61.7(π); 63.6(σ); 2382.2(σ);[c] 2397.5(σ)[d]
QCISD	6-311+G(2d,Ryd)[f]	1.0643	1.0979	3.2268	3.0(σ); 54.1,55.2(π); 106.3,106.6(π); 2386.2(σ);[d] 2394.0(σ)[c]

[a]$sp=0.025$ on NO only.
[b]*s*, 0.028; *p*, 0.025 on all N; *s*, 0.032; *p*, 0.028 on O.
[c]NO stretch.
[d]N_2 stretch.
[e]The Rydberg basis functions were *s*, 0.028; *p*, 0.025 on all N atoms; and *s*, 0.032; *p*, 0.028 on O.
[f]The Rydberg basis functions for N have exponents; *s*, 0.028, *p*, 0.025, *d*, 0.015; and for O: *s*, 0.032; *p*, 0.028, *d*, 0.015—from Ref. 34.

rotation of the NO (see Fig. 4). The conclusions are that NO is close to being freely rotating in the $\tilde{X}$ state. The highest energy isomers are the linear ones. In order to go from the T-shaped structures to the linear ones, N_2 must rotate in-plane—the higher energy indicates that N_2 is not so freely rotating as NO. The two linear isomers are linked by in-plane rotation of the NO. We note at this point that accurate vibrational frequencies would aid considerably in knowing how floppy the $\{NO\}\cdot N_2$ complex is in the $\tilde{X}$ state; however, such accurate frequencies would be prohibitively expensive to calculate. Probably the way forward will be to calculate an accurate potential energy surface (which will be expensive), and to derive the amplitudes of the motions of the atoms from it. At the present time, the description of the floppiness of the complex must remain qualitative, and must be viewed with some caution.

The floppy nature of the ground state suggests that one will be able to access a range of upper state geometries with reasonable intensity, owing to the amplitude of the ground state wavefunction over a wide angular range. As noted above, the simple nature of the origin feature suggests that the $\tilde{A}$ state is linear or close to it. To investigate this further, calculations on the $\tilde{A}^2\Sigma^+$ state were performed on the two linear isomers (for details, see Sec. III), $NO\cdot N_2$ and $ON\cdot N_2$. As was noted above, the most stable isomer was the $ON\cdot N_2$ isomer, with a binding energy of ca. 230 cm^{-1}. This is significantly larger than the experimental D_0' value, but zero-point vibrational energy will lower the calculated binding energy, although not by the extent required. In addition, the vibrational frequencies of the lowest energy isomer do not agree well with the observed ones; interestingly, however,

TABLE VI. Optimized geometries and harmonic vibrational frequencies of the linear $NO\cdot N_2$ $\tilde{A}^2\Sigma^+$ isomer at different levels of theory.

Method	Basis	r_{ON}/Å	r_{NN}/Å	$r_{O\cdots N}$/Å	Frequencies/cm^{-1}
MP2	6-31+G*(s,Ryd)[a]	1.0894	1.1307	3.4127	18.0(σ); 66.7(π); 102.6(π); 2346.3(σ);[b] 4345.1(σ)[c]
QCISD	As above	1.0849	1.1149	3.2974	d
QCISD	6-31+G*(Ryd)[e]	1.0842	1.1147	3.2862	1.8,2.2(π); 19.6(σ); 69.3, 69.4(π); 2356.1(σ);[b] 2397.2 (σ)[c]
QCISD	6-311+G(2d,Ryd)[e]	1.0644	1.0981	3.3995	21.7(σ); 66.7,66.9(π); 112.3,112.4(π); 2383.7(σ);[c] 2392.9(σ)[b]

[a]The Rydberg basis functions were: *s*, 0.028; *p*, 0.025 on all N atoms; and *s*, 0.032; *p*, 0.028 on O.
[b]NO stretch.
[c]N_2 stretch.
[d]Excessive QCISD iterations in the numerical second derivatives calculation.
[e]The Rydberg basis functions for N have exponents *s*, 0.028; *p*, 0.025; *d*, 0.015; and for O: *s*, 0.032; *p*, 0.028; *d*, 0.015—from Ref. 34.

Downloaded 17 Nov 2009 to 152.78.208.72. Redistribution subject to AIP license or copyright; see http://jcp.aip.org/jcp/copyright.jsp

those of the higher isomer do. It seems unlikely that the energy ordering of the two isomers will change at a higher level of theory, although it is plausible that the interaction of the $\tilde{A}^2\Sigma^+$ state with higher-lying states (such as the $\tilde{D}^2\Sigma^+$ state arising from the $3p\sigma$ NO orbital) might cause this. Another interpretation would be that only the higher energy $\tilde{A}$ state isomer is accessed in the transition, which would seem to imply that transitions from the ground state occur at geometries that favor a good overlap with its $NO\cdot N_2$ orientation. It is certainly not possible to rule out completely that there is more than one isomer populated in the supersonic expansion here, and that it is not the lowest one that gives rise to the spectrum; although the stability of the appearance of the spectrum under different expansion conditions makes this seem unlikely. Note that, in the absence of any detailed knowledge of the nonlinear regions of the potential energy surface of the $\tilde{A}$ state, and also in the absence of a reliable value for the calculated dissociation energy, a discussion of the details of the observed spectrum must remain tentative.

If the $\tilde{A}$ state of the $\{NO\}\cdot N_2$ complex is linear and fairly rigid as the calculated and experimental dissociation energies imply, then it will resemble a linear molecule close to the potential energy minimum with well-defined stretch and bend vibrations. (In principle, there will also be bend vibrational energy levels of the other linear isomer also, which will be higher in energy, but because of the large BSSE, it is unclear from the calculations how bound this state is.) As the stretch vibration is excited, the anisotropy felt by each diatomic owing to the presence of the other decreases as the average intermolecular separation increases. Eventually the anisotropy is low enough that each moiety can undergo hindered, and eventually free, internal rotation. In the nomenclature of Dubernet *et al.*,[37] near the minimum of the $\tilde{A}$ state there is a large (radially averaged) V_{10} term, which corresponds to the two linear isomers being widely separated in energy, and close to the origin there is also a large (radially averaged) negative V_{20} term, which corresponds to the molecule being fairly rigidly linear. As the anisotropy decreases, $|V_{20}|$ gets closer to zero, and eventually at $V_{20}=0$, the two moieties are freely rotating, each with its own internal rotation quantum number; the motion of these two rotors may then couple to each other, as well as to the overall rotation of the complex. The complexity of the spectrum to higher energy suggests that fairly-free rotation is occurring, and indeed it is possible to pick out some spacings that might be plausibly assigned to free rotor levels of NO; however, this is somewhat arbitrary, and a fuller modeling of the spectroscopy occurring will be required before the features to higher energy can be assigned with any certainty. Indeed, in this region overtones and combination bands are also expected to be present, increasing the difficulty further. This qualitative picture of the gradual unlocking of the rotation of the moieties mirrors the behavior we observed recently for the $Ar\cdot NO$ $\tilde{A}$ state.[9]

That the geometry of the $\tilde{A}$ state of $\{NO\}\cdot N_2$ is expected to be fairly rigid and close to linear, but the ground state is expected to be rather floppy both in- and out-of-plane explains the fact that a fair amount of vibrational excitation is observed in the spectrum. It is expected that the change from floppy bent to rigid linear will excite bending modes of the $\tilde{A}$ state, and the expected increase in binding energy will lead to a shorter intermolecular bond (as calculated) and thus excitation of the intermolecular stretch.

B. Comparison of the $\tilde{X}$ state with similar complexes

In Ref. 12, a discussion of the expected geometry of the $\tilde{X}$ state was presented, with comparisons to similar molecules, such as $(NO)_2$, $(NO)_2^+$ and $N_2\cdot CO$ being made. $(NO)_2^+$ is isoelectronic with $\{NO\}\cdot N_2$ and has been the focus of some attention,[38] but the presence of the positive charge precludes a direct comparison; $(NO)_2$ appears to have unusual bonding between the two N atoms. $N_2\cdot CO$ has been found to have a T-shaped structure from infrared absorption spectroscopy,[39–41] with the N_2 pointing towards the CO bond, but there is disagreement with theoretical calculations.[42] In addition, the infrared study concluded that the CO was loosely bound and nearly freely rotating—this appears to be similar to the case here where NO is concluded to be close to freely rotating. The similarity of the NO dipole and quadrupole moments [0.157 D, 2.4×10^{-26} esu cm^2] to those of CO[0.1098 D, 2.0×10^{-26} esu cm^2] must contribute to these conclusions, although the extra electron in NO must lead to some extra Pauli repulsion. This similarity of the dipole and quadrupole moments of NO and CO would lead to the expectation that the binding energies of $\{NO\}\cdot N_2$ and $N_2\cdot CO$ would be fairly similar, and indeed Xia *et al.*[41] have roughly estimated (from the results of previously reported *ab initio* calculations) that D_0 for $N_2\cdot CO$ is ca. 90 cm^{-1}, which is about the same as the values derived herein.

Recently, work has been presented also on the CO dimer,[43,44] and it has been deduced from the results of *ab initio* calculations[45] that there is fluctional behavior, owing to a number of energetically close minima, below the expected zero-point level. Very recently, it has been noted[46] that high-order contributions are important in the determination of the binding energy of the CO dimer, and that even the CCSD(T) method may not be sufficient. The $(N_2)_2$ molecule would be another good comparison; however, experimentally this has proven difficult to study, owing to the absence of an allowed dipole transition; *ab initio* studies indicate a similar picture, however.[47] We note in passing that in Ref. 47, although the level of calculation performed on $(N_2)_2$ was high, [CCSD(T)/cc-pVQZ], no diffuse functions appear to have been included in the basis set, which clearly would limit the accuracy of the calculated potential energy surface. An earlier study by Stallcop and Partridge[48] (not cited in Ref. 47) employed the aug-cc-pVQZ basis set, with different sets of diffuse functions, and even employed the cc-pV5Z basis set (without the *h* functions).

These studies, in combination with the ones reported herein, have a profound implication for the calculation of the potential energy surface of the $\tilde{X}$ state of the $\{NO\}\cdot N_2$ complex. First, it would seem that at least the CCSD(T) method is required, and that a basis set of aug-cc-pVQZ quality is necessary. This, in itself, makes such a calculation expensive. In addition, the mapping out of the potential energy

Downloaded 17 Nov 2009 to 152.78.208.72. Redistribution subject to AIP license or copyright; see http://jcp.aip.org/jcp/copyright.jsp

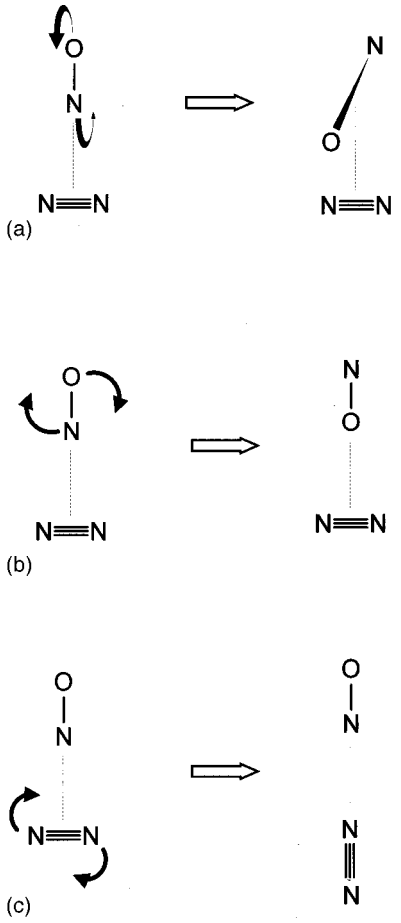

FIG. 4. Schematic diagram showing the motions that lead from a T-shaped $ON\cdot N_2$ geometry to (a) the ''X''-shaped geometry; (b) the T-shaped $NO\cdot N_2$ geometry; and (c) the linear $ON\cdot N_2$ geometry.

surface, even under the assumption that the NO and N_2 vibrations may be factored out, requires variation in four variables (the center-of-mass separation, and the two in-plane angles of the two diatoms, and the out-of-plane angle). Such a mapping must be performed for the two states arising from the unpaired electron of NO being ''in-plane'' and ''out-of-plane,'' and each energy point needs to be corrected for BSSE. Clearly, such a calculation, although perfectly feasible, will require a large amount of computational effort.

For the $\tilde{A}$ state, things are less complicated since this electronic state is nondegenerate, but as discussed above, converging the calculation to the correct state is not trivial for nonlinear orientations, and a MRCI approach would appear to be required.

Clearly, a detailed understanding of the $\tilde{A}\leftarrow\tilde{X}$ transition of $\{NO\}\cdot N_2$ is going to require a concerted attack: the calculation of reliable surfaces for both the $\tilde{X}$ and $\tilde{A}$ state and the recording of higher-resolution electronic spectra. Trends in the derived rotational constants should help to identify progressions from the overall spectrum recorded. We note that some progress has been made in the recording of such high-resolution spectra of $\{NO\}\cdot N_2$ by high-resolution laser induced fluorescence, but the analysis has not yet been performed.[49] The interpretation of the latter will be challenging, since the details of the angular momentum coupling will need to be considered. We note that in the $\tilde{X}^2\Pi$ state, the orbital and spin angular momenta of the unpaired electron on NO will be coupled to the NO molecular axis (Hund's case a), and the sum of their projections (ω) will couple with the internal rotation angular momentum of the NO(r_{NO}), to form a resultant (j_{NO}); N_2 will also have an internal rotation quantum number, r_{N_2}, which will couple to the intermolecular axis. At this point, consideration must then be given as to how j_{NO}, r_{N_2} and the end-over-end rotation of the complex as a whole couple to form the overall angular momentum, J. Coriolis coupling and spin-rotation may also have to be considered in order to gain a good fit of the spectrum, and nuclear spin effects may also be apparent: the latter have been observed in $N_2\cdot CO$[41] where *ortho* and *para* forms have been identified.

Microwave and/or infrared spectroscopic studies would also be of great use in elucidating the structure of the $\tilde{X}$ state.

C. $\{NO\}^+\cdot N_2$

$\{NO\}^+\cdot N_2$ has been studied recently using *ab initio* calculations,[50,51] and is found to have a skewed T-shaped structure with the N_2 pointing towards the NO center-of-mass. The binding energy was estimated to be 1950 cm^{-1}, which is far greater than that of the $\tilde{X}$ or $\tilde{A}$ states. This disparity in binding energies indicates that the N_2 molecule lies outside the orbit of the 3*s* Rydberg electron of NO in the neutral complex. Higher electronic states, where the unpaired electron of NO has been promoted to higher-*n* orbitals, are expected to have much greater binding energies, as the Rydberg orbital becomes large enough to accommodate the N_2 molecule, leading to a Rydberg state of $NO\cdot N_2$, rather than a N_2 molecule interacting with a Rydberg state of NO.

VI. CONCLUSIONS

We have presented two separate studies in the present paper: a study of the (1+1) REMPI spectrum of NO complexed to N_2, and a detailed set of calculations on the $\tilde{X}$ state of the $\{NO\}\cdot N_2$ complex. In addition, based upon the appearance of the REMPI spectrum, a set of calculations on the two linear isomers of the $\tilde{A}$ state were also reported.

The appearance of the REMPI spectrum of the $\tilde{A}\leftarrow\tilde{X}$ transition of $\{NO\}\cdot N_2$ under a variety of conditions leads to the conclusion that there is only one contributor to the observed spectrum. High-level *ab initio* calculations indicate that the global minimum on the $\tilde{X}$ state potential energy surface is an ''X''-shaped structure, but that there are at least seven minima very close in energy, some of which are liable to be accessible with zero-point vibrational energy. It is probable that the $\{NO\}\cdot N_2$ complex will sample a wide range of geometries, even at the low energies of the molecular beam used here. These conclusions are consistent with conclusions reached by other workers on the related complexes $(CO)_2$ and $N_2\cdot CO$. The simple appearance of the low-energy region of the REMPI spectrum indicates that the $\tilde{A}$ state is probably linear, with a binding energy of 130–145 cm^{-1}. Even with the high-level of calculations presented here, it was not possible to be conclusive about the details of

Downloaded 17 Nov 2009 to 152.78.208.72. Redistribution subject to AIP license or copyright; see http://jcp.aip.org/jcp/copyright.jsp

the assignment of the spectrum. Further experimental and theoretical work on this complex are warranted, to characterize both the ground and excited states better. Given the progress that has been made in recording the microwave and infrared spectra of related species, it will only be a matter of time before the ground state is much better understood. As noted above, some higher-resolution LIF spectra of the $\tilde{A} \leftarrow \tilde{X}$ transition are available, but their interpretation will probably be demanding.

ACKNOWLEDGMENTS

We are grateful to EPSRC and NERC for funding. The authors are grateful to the EPSRC for the award of computer time at the Rutherford Appleton Laboratories, which enabled the calculations to be performed. E.P.F.L. is grateful to the Research Grant Council (RGC) of the Hong Kong Special Administration Region (HKSAR) and the Research Committee of the Hong Kong Polytechnic University for support. T.G.W. is grateful to the EPSRC for the award of an Advanced Fellowship.

[1] M. C. Heaven, Annu. Rev. Phys. Chem. **43**, 283 (1992).
[2] M. C. Heaven, J. Phys. Chem. **97**, 8567 (1993).
[3] X. Q. Tan, T. G. Wright, and T. A. Miller, in *Jet Spectroscopy and Molecular Dynamics*, edited by J. M. Hollas and D. Phillips (Blackie, London, 1995).
[4] C. C. Carter, H.-S. Lee, A. B. McCoy, and T. A. Miller, J. Mol. Struct. **525**, 1 (2000), and references therein.
[5] H. Meyer, J. Chem. Phys. **107**, 7732 (1997).
[6] P. Mack, J. M. Dyke, D. M. Smith, T. G. Wright, and H. Meyer, J. Chem. Phys. **109**, 4361 (1998).
[7] J. Fleniken, Y. Kim, and H. Meyer, J. Chem. Phys. **109**, 8940 (1998).
[8] S. D. Gamblin, S. E. Daire, J. Lozeille, and T. G. Wright, Chem. Phys. Lett. **325**, 232 (2000).
[9] J. Lozeille, S. E. Daire, S. D. Gamblin, T. G. Wright, and D. M. Smith, J. Chem. Phys. **113**, 7224 (2000).
[10] See, R. A. Loomis and M. I. Lester, Annu. Rev. Phys. Chem. **48**, 643 (1997), and references therein.
[11] M. Tsiouris, M. D. Wheeler, and M. I. Lester, Chem. Phys. Lett. **302**, 192 (1999).
[12] P. Mack, J. M. Dyke, D. M. Smith, and T. G. Wright, Chem. Phys. Lett. **284**, 423 (1998).
[13] J. C. Miller, J. Chem. Phys. **86**, 3166 (1987).
[14] M. Akiike, K. Tsuji, K. Shibuya, and K. Obi, Chem. Phys. Lett. **243**, 89 (1995).
[15] S. E. Daire, J. Lozeille, S. D. Gamblin, and T. G. Wright, J. Phys. Chem. A **104**, 9180 (2000).
[16] P. D. A. Mills, D. Phil. thesis, Oxford, 1983.
[17] B. J. Howard (personal communication).
[18] P. D. A. Mills, C. M. Western, and B. J. Howard, J. Phys. Chem. **90**, 4961 (1986).
[19] Y. Kim, J. Fleniken, and H. Meyer, J. Chem. Phys. (manuscript submitted).
[20] M. H. Alexander, P. Soldán, T. G. Wright, Y. Kim, H. Meyer, P. J. Dagdigian, and E. P. F. Lee (manuscript submitted).
[21] Y. Kim, K. Patton, Y. Fleniken, and H. Meyer, Chem. Phys. Lett. **318**, 522 (2000).
[22] Y. Kim, J. Fleniken, H. Meyer, P. J. Dagdigian, and M. H. Alexander, J. Chem. Phys. **112**, 4952 (2000).
[23] W. M. Fawzy, G. T. Fraser, J. T. Hougen, and A. S. Pine, J. Chem. Phys. **93**, 2992 (1990).
[24] C. R. Dennis, C. J. Whitham, R. J. Low, and B. J. Howard, Chem. Phys. Lett. **282**, 421 (1998).
[25] J. Kłos, H. Chałasiński, M. T. Berry, R. Bukowski, and S. M. Cybulski, J. Chem. Phys. **112**, 2195 (2000).
[26] M. H. Alexander, J. Chem. Phys. **111**, 7426 (1999); **111**, 7435 (1999).
[27] D. W. Ball, J. Phys. Chem. A **101**, 4835 (1997).
[28] G. Myszkiewicz and J. Sadlej, Chem. Phys. Lett. **318**, 232 (2000).
[29] J. Danielak, U. Domin, R. Kepa, M. Rytel, and M. Zachwieja, J. Mol. Spectrosc. **181**, 394 (1997).
[30] R. Engelmann, Jr., P. E. Rouse, H. M. Peek, and V. D. Baiamonte, ''The beta and gamma band systems of nitric oxide,'' Los Alamos Scientific Laboratory Report LA-4364, 1970.
[31] S. J. Boys and F. Bernardi, Mol. Phys. **19**, 553 (1970).
[32] GAUSSIAN98, M. J. Frisch *et al.* (Gaussian Inc., Pittsburgh, 1998).
[33] MOLPRO is a package of *ab initio* programs written by H.-J. Werner and P. J. Knowles, with contributions from J. Almlöf, R. D. Amos, A. Berning *et al.*, with the CCSD treatment being described in C. Hampel, K. Peterson, and H.-J. Werner, Chem. Phys. Lett. **190**, 1 (1992).
[34] T. H. Dunning and P. J. Hay, in *Modern Theoretical Chemistry*, edited by H. F. Schaefer III (Plenum, New York, 1977), Vol. 2.
[35] K. Tsuji, K. Shibuya, and K. Obi, J. Chem. Phys. **100**, 5441 (1994).
[36] G. Herzberg, *Molecular Spectra and Molecular Structure I: Spectra of Diatomic Molecules* (Krieger, Malabar, 1991).
[37] M.-L. Dubernet, D. Flower, and J. M. Hutson, J. Chem. Phys. **94**, 7602 (1991).
[38] Y. Xie and H. F. Schaefer III, Mol. Phys. **98**, 955 (2000), and references therein.
[39] Y. Kawashima and K. Nishizawa, Chem. Phys. Lett. **249**, 87 (1996).
[40] Y. Xu and A. R. W. McKellar, J. Chem. Phys. **104**, 2488 (1996).
[41] C. Xia, A. R. W. McKellar, and Y. Xu, J. Chem. Phys. **113**, 525 (2000), and references therein.
[42] K. A. Franken and C. E. Dykstra, J. Phys. Chem. **97**, 11408 (1993).
[43] Y. Xu and W. Jäger, J. Chem. Phys. **111**, 5754 (1999).
[44] M. D. Brookes and A. R. W. McKellar, J. Chem. Phys. **111**, 7321 (1999).
[45] A. W. Meredith and A. J. Stone, J. Phys. Chem. **102**, 434 (1998).
[46] M. Rode, J. Sadlej, R. Moszynki, P. E. S. Wormer, and A. van der Avoird, Chem. Phys. Lett. **314**, 326 (1999).
[47] A. Wada, H. Kanamori, and S. Iwata, J. Chem. Phys. **109**, 9434 (1998).
[48] J. R. Stallcop and H. Partridge, Chem. Phys. Lett. **281**, 212 (1997).
[49] C. C. Carter, T. A. Miller, J. Lozeille, and T. G. Wright, work in progress.
[50] P. Mack, J. M. Dyke, and T. G. Wright, Chem. Phys. **218**, 243 (1997).
[51] P. Soldán, E. P. F. Lee, L. A. Jones, and T. G. Wright, J. Phys. Chem. A **103**, 5547 (1999).

Downloaded 17 Nov 2009 to 152.78.208.72. Redistribution subject to AIP license or copyright; see http://jcp.aip.org/jcp/copyright.jsp